I&EC research
Industrial & Engineering Chemistry Research

Article

pubs.acs.org/IECR

Controlling and Formation Mechanism of Oxygen-Containing Groups on Graphite Oxide

Zhiting Liu, Xuezhi Duan, Xinggui Zhou, Gang Qian, Jinghong Zhou,* and Weikang Yuan

State Key Laboratory of Chemical Engineering, East China University of Science and Technology, 130 Meilong Road, Shanghai, 200237, People's Republic of China

Supporting Information

ABSTRACT: Controllable synthesis of graphite oxide (GO) for targeted surface properties is of great importance for its versatile applications. For this purpose, GO samples were prepared with different amounts of oxidant and characterized by X-ray diffraction, Fourier transform infrared spectroscopy, ^{13}C cross-polarization with total sideband suppression magic-angle-spinning nuclear magnetic resonance, X-ray photoelectron spectroscopy, Raman spectroscopy, and ζ-potential measurement. When the oxidant amount is below a critical value, the epoxy groups are dominant on the GO surfaces, together with a few hydroxyl and carbonyl groups. Further increase in the oxidant amount leads to the formation and development of the carboxyl groups, which eventually reach a saturation level. Meanwhile, the increasing oxygen-containing groups introduce more defects and reduce the crystalline graphene domains on GO. A possible mechanism for the formation of the oxygen-containing groups on GO is proposed, providing a guideline for the manipulation of the GO surface properties.

1. INTRODUCTION

Engineering the oxygen-containing groups of graphite oxide (GO) to desirable physicochemical properties has long been actively engaged.[1,2] This is because many applications of GO such as the graphene precursor,[3−6] adsorbent,[7−10] or metal-free catalyst[11−13] are highly dependent on the sp^2/sp^3 ratio and the oxygen-containing groups. For instance, the carboxyl groups at the edges of GO and the epoxy groups on the basal planes have a good adsorption performance for NH_3 molecules.[14] The epoxy groups on GO are active sites for selective oxidation of alcohols to aldehydes, oxidative dehydrogenation of propane to propene, and polymerization of various olefin monomers.[15,16] The carboxyl and epoxy groups on graphene can easily react with functionalized groups such as amino groups and hydroxyl groups and can be used to prepare functionalized graphene and graphene-based composites.[17−20] However, in the case of graphene preparation, the carboxyl groups left at the edges of GO will lower the yield of graphene when subjected to high temperature for reduction. Moreover, the carboxyl groups cannot be effectively or efficiently reduced by the commonly used reductants such as hydrazine and sodium borohydride.[21,22] Therefore, understanding the formation mechanism of oxygen-containing groups on GO to manipulate its properties is very important for its versatile applications.

Brodie's, Staudenmaier's, Hummers', and their modified methods are most frequently used to prepare GO, which involve oxidation of graphite with a mixture of strong oxidant (e.g., $KClO_3$ or $KMnO_4$) and strong acid (e.g., fuming HNO_3 or concentrated H_2SO_4).[23] Many attempts have been made to characterize the oxygen-containing groups on GO and unveil the structure of GO,[24−33] in which there is a widespread consensus that the hydroxyl and epoxy groups are located on the basal planes and the carboxyl and carbonyl groups are at the edges.[30,31b,34,35] However, in these studies, high oxidant/graphite weight ratios of more than 3 led to the fast and full development of the oxygen-containing groups[26−28,34,36] and, thus, controlling the oxygen-containing groups with difficulty. Furthermore, very little attention has been paid to the relative concentration distribution of the oxygen-containing groups on GO with the oxidation degree. This is limiting the understanding of the formation mechanism of the surface groups which provides a guideline for the manipulation of the surface properties of GO. With this perspective, it is essential to keep the oxidation degree under control during graphite oxidation in favor of observing the formation of the oxygen-containing groups on GO.

In this work, a modified Hummers' method was used to prepare GO by reacting graphite with a mixture of $KMnO_4$ and H_2SO_4. Considering the easy oxidation of the intermediate oxygen-containing groups, i.e., the ketone groups, we tuned the oxidation degree of GO by changing the weight ratio of $KMnO_4$/graphite (i.e., 6/3, 7/3, 10/3, and 15/3). The as-synthesized GO samples with the different oxidation degrees were characterized by X-ray diffraction (XRD), Fourier transform infrared spectroscopy (FTIR), ^{13}C cross-polarization with total sideband suppression magic-angle-spinning nuclear magnetic resonance (^{13}C CPTOSS/MAS NMR), X-ray photoelectron spectroscopy (XPS), Raman spectroscopy, and zeta (ζ) potential measurement, based on which the type and contents of the oxygen-containing groups on the GO samples were determined and the surface property was investigated. Accordingly, a possible mechanism for the formation and transformation of the oxygen-containing groups was proposed.

Received: September 17, 2013
Revised: December 6, 2013
Accepted: December 13, 2013
Published: December 13, 2013

dx.doi.org/10.1021/ie403088t | *Ind. Eng. Chem. Res.* 2014, 53, 253−258

2. EXPERIMENTAL SECTION

2.1. Preparation of GO. GO was synthesized by a modified Hummers' method.[37] First, graphite (12 g) was pretreated with concentrated H_2SO_4 (50 mL), $K_2S_2O_6$ (10 g), and P_2O_5 (10 g), and was subsequently washed and dried. The pretreated graphite (3 g), together with a specified amount of $KMnO_4$ (i.e., 6, 7, 10, and 15 g) was added to concentrated H_2SO_4 (115 mL) under agitation at 0 °C, and the as-obtained mixture was transferred to a water bath of 35 °C for 2 h, which was then dispersed in a 600 mL ice−water mixture. Finally, the mixture was treated with 30% H_2O_2 (12 mL), filtered, washed with 10% HCl aqueous solution (2 L) and then water until the filtrate was neutral, and dried in a vacuum oven at 35 °C for more than 2 days. The GO products prepared with $KMnO_4$/graphite weight ratios of 6/3, 7/3, 10/3, and 15/3 were designated as GO-1, GO-2, GO-3, and GO-4, respectively.

2.2. Characterization. The graphite and prepared GO samples were characterized with XRD (Rigaku D/Max2550VB/PC, Cu Kα radiation). The oxygen-containing groups on GO were identified with FTIR on a Magna-IR 550 (Nicolet, USA) where the samples were prepared in potassium bromide pellets, and with ^{13}C CPTOSS/MAS NMR at 11.5 T using a Bruker AVANCE 500 MHz spectrometer with 4 mm zirconia magic angle spinning rotors where the spectra were recorded with spinning at 125 MHz, 12 μs and 1 ms contact time. The chemical states and the elemental compositions of GO were studied with XPS (Kratos XSAM-800) using Al Kα ($h\upsilon$ 1486.6 eV) X-ray as the excitation source. The Raman spectra using excitation wavelength 514 nm were measured with an inVia Raman microscope (Renishaw, U.K.). The ζ potentials of the GO samples were determined with a Zetasizer Nanoseries Nano-ZS (Malvern) instrument.

3. RESULTS AND DISCUSSION

The XRD patterns of graphite and the GO samples prepared by using different $KMnO_4$/graphite weight ratios are shown in Figure 1. With the increase of the $KMnO_4$/graphite weight ratio from 6/3, 7/3, 10/3, to 15/3, the (002) peaks of graphite centering at 26.50° disappear gradually, while the (002) peaks of GO for all four GO samples are observed around 10°.[27,36] Specifically, the characteristic diffraction peaks of both GO and graphite are observed on GO-1, whereas no evident characteristic diffraction peak of graphite exists on the other samples, indicating that the oxidation does not complete until the $KMnO_4$/graphite weight ratio is increased to 7/3. Moreover, the (002) peak of GO shifts from 10.90 to 8.96° and the corresponding interplanar distance (d_{002}) increases from 8.11 to 9.86 nm as the weight ratio of $KMnO_4$/graphite is increased. The expansion of the interlayer distance of GO samples is due to the generation of oxygen-containing groups and the presence of adsorbed water between the hydrophilic graphene oxide layers.[28] These results indicate that a high weight ratio of $KMnO_4$/graphite facilitates the intercalation and oxidation of graphite. The different oxidation degrees of GO-1 to GO-4 are indicated by the colors of their aqueous dispersions, which change from black-brown to brown, as seen in the inset of Figure 1.

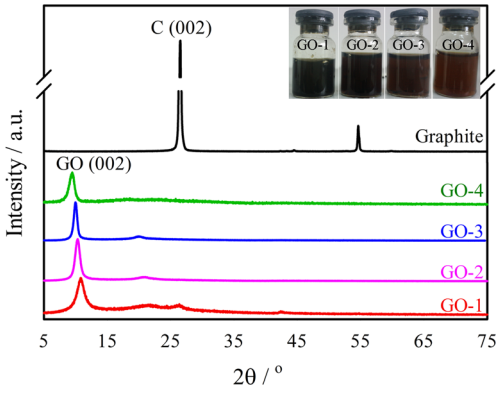

Figure 1. XRD patterns of graphite, GO-1, GO-2, GO-3, and GO-4. (inset) Photos of GO-1, GO-2, GO-3, and GO-4 aqueous dispersions at a concentration of 0.25 mg/mL.

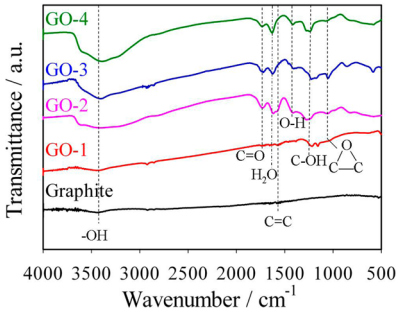

Figure 2. FTIR spectra of graphite, GO-1, GO-2, GO-3, and GO-4.

Table 1. FTIR Data of Graphite, GO-1, GO-2, GO-3, and GO-4

assignment	graphite	GO-1	GO-2	GO-3	GO-4
−OH str vibr	3433	3419	3409	3405	3409
C═O str vibr	–	1720	1723	1720	1735
H_2O def vibr	–	1637	1619	1624	1622
C═C str vibr	1565	1579	1583	–	–
O−H str vibr of COOH	–	–	1414	1406	1407
C−OH str vibr	–	1217	1223	1224	1223
C−O−C str vibr	–	1157	1055	1052	1097

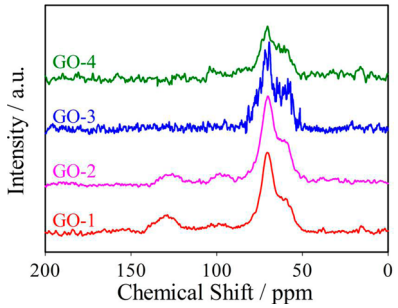

Figure 3. ^{13}C CPTOSS/MAS NMR spectra of GO-1, GO-2, GO-3, and GO-4.

Figure 2 shows the FTIR spectra of GO-1, GO-2, GO-3, and GO-4, and Table 1 summarizes the peak positions and their assignments. GO-1, which was prepared with a $KMnO_4$/graphite weight ratio of 6/3, has infrared absorption peaks centering at 1157, 1217, 1579, 1637, 1720, and 3419 cm^{-1}, which can be assigned to the C−O stretching vibration of the epoxy groups, the C−OH stretching vibration, the C═C bond stretching vibration, the adsorbed H_2O deformation vibration, the C═O stretching vibration, and the −OH stretching vibration of the adsorbed water and the hydroxyl groups, respectively.[14a,38,39] As a comparison, graphite has only two

dx.doi.org/10.1021/ie403088t | Ind. Eng. Chem. Res. 2014, 53, 253−258

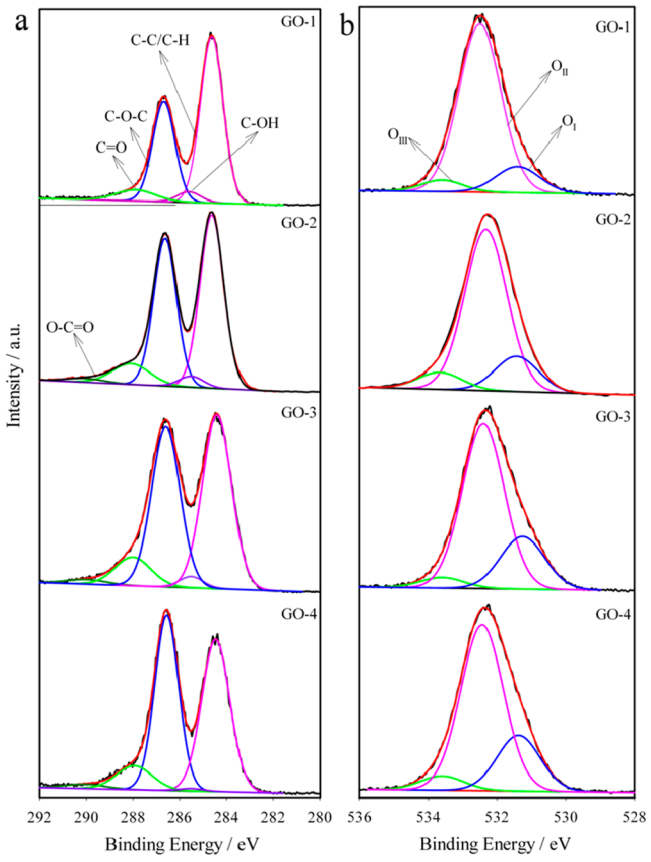

Figure 4. (a) C 1s and (b) O 1s XPS spectra of GO-1, GO-2, GO-3, and GO-4.

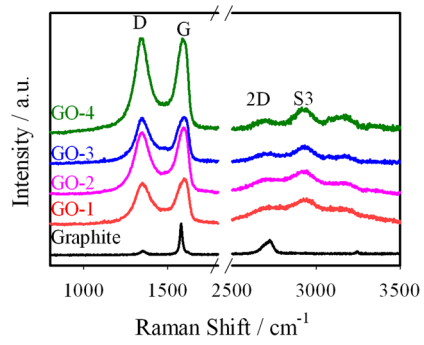

Figure 5. Raman spectra of graphite, GO-1, GO-2, GO-3, and GO-4.

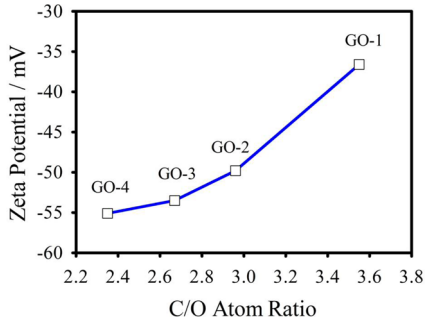

Figure 6. ζ potentials of GO-1, GO-2, GO-3, and GO-4 aqueous dispersions as a function of C/O atom ratio.

weak absorption peaks due to C═C bonds, absorbed water and hydroxyl groups. The O−H stretching vibration of the carboxyl groups around 1400 cm^{-1} is not observed on GO-1,[32,38,39] and the absorption peak of C═O around 1720 cm^{-1} is very weak, indicating that the carboxyl groups have not been developed because of the insufficient oxidant. However, the peak at 1414 cm^{-1} owing to the O−H stretching vibrations of the carboxyl groups appears on GO-2, and the peak at 1720 cm^{-1} becomes stronger. This indicates that the carboxyl groups have been formed after the increase of the $KMnO_4$/graphite weight ratio to 7/3. This fact also manifests that the carboxyl groups are formed in the last stage of oxidation when enough oxidant is used. It is worth noting that on GO-1 and GO-2 there exist unoxidized aromatic domains, as revealed by the peak centering at 1565−1583 cm^{-1} which is assigned to the stretching of C═C bonds.[32,39] However, this peak disappears on GO-3 and GO-4, indicating that the surface of graphene is sufficiently oxidized.

Figure 3 shows the ^{13}C CPTOSS/MAS NMR spectra of the GO samples. The three main peaks in GO centering around 60, 70, and 130 ppm are assigned to the epoxy, hydroxyl, and C═C bonds, respectively.[26,40,41] The peak intensities of the hydroxyl groups are most significant owing to the cross-polarization by the proton in the hydroxyl groups.[26] With the increase of the degree of oxidation, the peak intensity of the hydroxyl groups becomes weaker, while that of epoxy groups becomes stronger. Simultaneously, the peaks of C═C bonds gradually disappear for GO-3 and GO-4; this observation is consistent with the FTIR characterization. It indicates that part of the hydroxyl groups may condense to the epoxy groups by dehydration reaction and/or be further oxidized to other oxygen-containing groups. However, no bands attributed to the carbonyl and carboxyl groups in all GO samples are observed under NMR detection, which is because of the low concentrations of these groups.[40]

To quantitatively indicate the surface states of the GO samples, the C 1s and O 1s XPS spectra are fitted with Gaussian curves as shown in Figure 4. The C/O atomic ratios for GO-1, GO-2, GO-3, and GO-4 calculated from the corresponding peak areas of the XPS are determined as 3.55, 2.96, 2.67, and 2.35, respectively, showing quantitatively the elevated oxidation degree of the GO with the increased amount of oxidant. As shown in Figure 4a and Table S1 in the Supporting Information, for a low $KMnO_4$/graphite weight ratio of 6/3, there exist four distinct Gaussian peaks in GO-1 centering at 284.6, 285.5, 286.6, and 280.0 eV, corresponding to C−C/C−H, C−OH, C−O−C, and C═O, respectively.[42,43]

Table 2. Chemical States of C and O Atoms on GO-1, GO-2, GO-3, and GO-4 with Their Relative Atomic Concentrations (atom %)

samples	C−C/C−H	C−OH	C−O−C	C═O	O═C−O	O_I	O_{II}	O_{III}
GO-1	56.2	3.8	33.4	6.6	–	13.1	81.4	5.5
GO-2	47.3	3.4	39.5	8.5	1.3	16.7	75.1	8.2
GO-3	45.7	2.4	41.1	9.2	1.7	23.8	71.4	4.8
GO-4	44.7	0.6	43.9	9.0	1.8	23.7	70.2	6.1

dx.doi.org/10.1021/ie403088t | Ind. Eng. Chem. Res. 2014, 53, 253−258

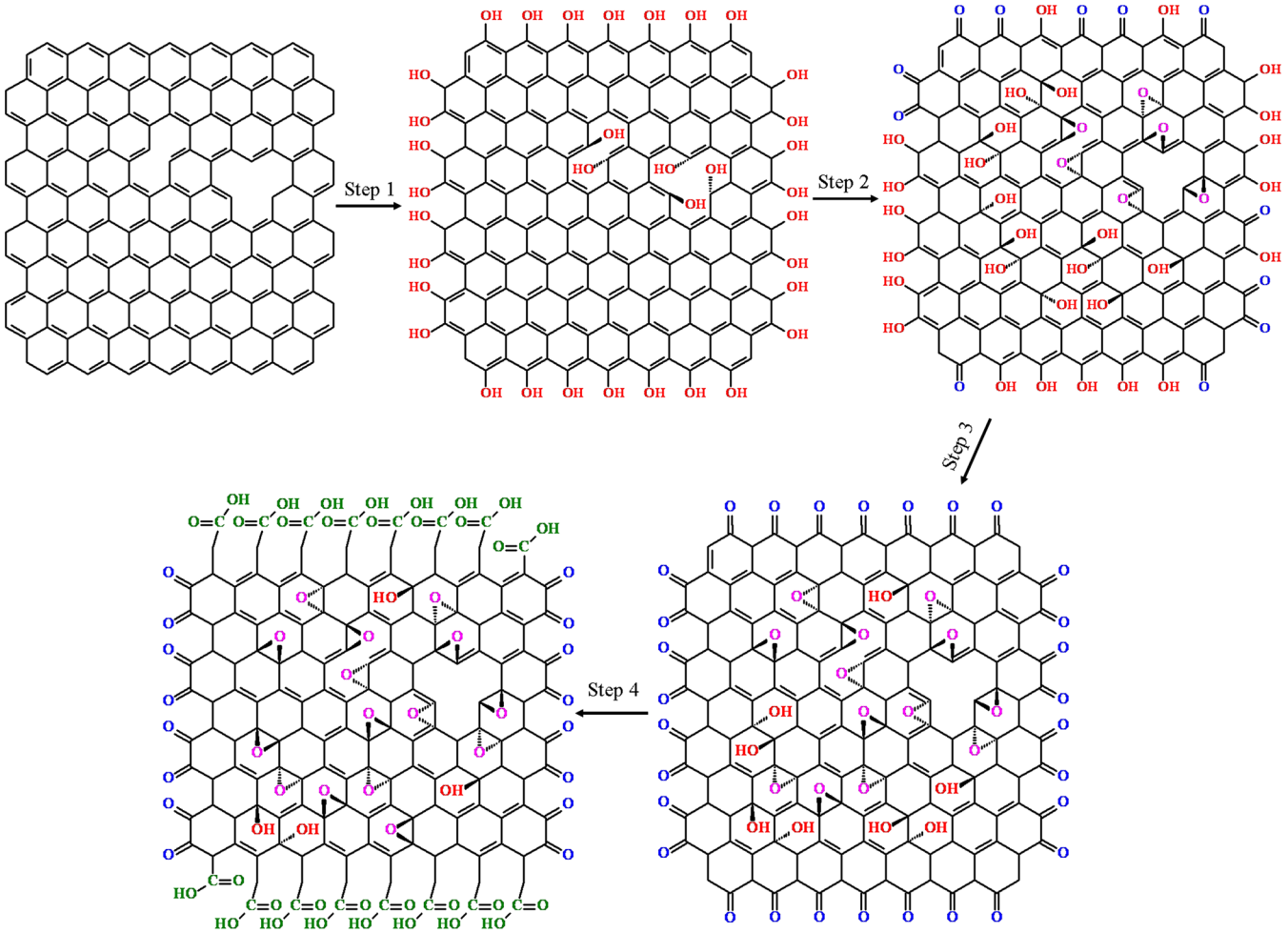

Figure 7. Diagram of the formation of the oxygen-containing groups on GO.

While for high $KMnO_4$/graphite weight ratios of 7/3, 10/3, and 15/3 (i.e., GO-2, GO-3, and GO-4), besides C−C/C−H (284.6/284.4/284.5), C−OH (285.5), C−O−C (286.6), and C═O (288.0) peaks, there is another peak centering at 290.1 eV corresponding to O═C—O. These observations agree well with the results of FTIR that the carboxyl groups are developed only with high $KMnO_4$/graphite weight ratios.

Table 2 shows the relative concentrations of the various oxygen-containing groups of the GO samples estimated from their respective fitting peak areas. From GO-1 to GO-4, the relative atomic concentration of the hydroxyl groups decreases, while those of the epoxy, carbonyl, and carboxyl groups increase with increased $KMnO_4$/graphite weight ratios, which is in line with the results of NMR and an indication of the conversion of the hydroxyl groups to the epoxy, carbonyl, and carboxyl groups. It is worth noting that the amounts of the carbonyl and carboxyl groups almost remain unchanged as the $KMnO_4$/graphite weight ratio is higher than 7/3, as revealed by the equal carbonyl and carboxyl group concentrations on GO-3 and GO-4. This is further confirmed by the O 1s XPS spectra of GO-1, GO-2, GO-3, and GO-4. As shown in Figure 4b, the O_I peak at 531.3/531.4 eV is assigned to oxygen atoms from C═O in carboxyl or carbonyl groups, the O_{II} peak at 532.4/532.5 eV is assigned to C−O in epoxy, hydroxyl, or carboxyl groups, and the O_{III} peak at 533.6 eV is assigned to oxygen atoms in water and/or chemisorbed oxygen species.[14a] In agreement with the results of C 1s XPS spectra, the relative concentration of oxygen atoms from C═O on these four GO samples first increases and then remains unchanged. The presence of the saturation values of carbonyl and carboxyl groups from C 1s and O 1s XPS spectra provides a good indication of complete oxidation of the edges that form carbonyl and carboxyl groups.

Raman spectra of graphite, GO-1, GO-2, GO-3, and GO-4 are shown in Figure 5. For the graphite, the presence of the D band indicates that there exist defects on it, which are prone to be attacked by oxidant. Furthermore, the Raman D/G and 2D/S3 intensity ratios (I_D/I_G and I_{S3}/I_{2D}) are usually used to evaluate the average sizes of crystalline sp^2 domains and defect densities in graphene sheets.[44,45] The I_D/I_G ratios are 0.88, 0.92, 1.00, and 1.02, and I_{S3}/I_{2D} ratios are 1.27, 1.35, 1.75, and 1.82 for GO-1, GO-2, GO-3, and GO-4, respectively. The increase of the I_D/I_G and I_{S3}/I_{2D} ratios from GO-1, GO-2, GO-3, to GO-4 suggests that increasing the oxygen-containing groups introduces more defects and reduces the crystalline graphene domains on the GO.[46]

Figure 6 shows the ζ potentials of GO-1, GO-2, GO-3, and GO-4 aqueous dispersions, which are all negative because of the ionization of the oxygen-containing groups. GO-2, GO-3, and GO-4 are more negative and hence more stable in aqueous dispersion, which is because of the increased oxidation degree, especially the increased carboxyl group concentration on GO. Because the carboxyl groups are unlikely to be completely reduced by hydrazine or $NaBH_4$, they will remain in the reduced products and prevent the aggregation of graphene

dx.doi.org/10.1021/ie403088t | Ind. Eng. Chem. Res. 2014, 53, 253−258

layers.[21] When producing graphene from GO-1, a surfactant should be used to stabilize the reduced graphene in solution.

According to the above investigation, we propose the formation mechanism of the oxygen-containing groups shown in Figure 7. First, oxidation attack is first on the carbon atoms at the edges or defects of graphene layers, which forms the hydroxyl groups. With the progress of oxidation, more hydroxyl groups are generated on the basal planes. Simultaneously, the formed hydroxyl groups at the edges are further oxidized to the carbonyl groups in the forms of the ketone and/or quinone groups, and the neighboring hydroxyl groups on the basal planes condense to the epoxy groups by dehydration in the strong acid environment. Subsequently, the ketone groups at the edges are further oxidized to the carboxyl groups with the six-member carbon ring opening in the presence of excess $KMnO_4$ and concentrated H_2SO_4, which is relatively slower compared with the formation of the carbonyl groups. After all the edges of graphite are oxidized, the carbonyl and carboxyl groups reach their saturation and their concentrations remain unchanged. In general, the electron donating groups (i.e., hydroxyl and epoxy) form first, while the electron withdrawing groups (i.e., the carbonyl and carboxyl groups) appear later. It is important to note that the carboxyl groups do not develop when a small amount of oxidant is used, because the oxidant is consumed by the precedent fast oxidation process. This is a strong indication of the sequential, step-by-step mechanism of graphene oxidation. Parallel to the sequential oxidation is the dehydration that forms the epoxy groups once the neighboring hydroxyl groups emerge. Moreover, the increase of the oxygen-containing groups on GO promotes the formation of more relatively small sp^2 carbon clusters and defects.

4. CONCLUSION

In this work, we demonstrate how the oxygen-containing groups on GO change with the amount of oxidant in the modified Hummers method. Oxidation first takes places at the edges or defects of graphene layers and produces the hydroxyl groups, immediately after which further oxidation of the hydroxyl groups to the carbonyl groups and dehydration of the hydroxyl groups to the epoxy groups take place in parallel. Though the concentrations of the carbonyl and epoxy groups will increase with the amount of oxidant, the carboxyl groups will not form until the dosing of oxidant is above a critical amount. Above this critical value, the ketone groups will be oxidized to the carboxyl groups, while the quinone groups are inactive and remain at a constant concentration. Further increasing the amount of oxidant above this critical value will produce more carboxyl groups, but when all the ketone groups are oxidized, no more carboxyl groups will be formed. Hereafter, except for the dehydration of the hydroxyl groups to form the epoxy groups, no appreciable oxidation occurs and the carboxyl groups, like the quinone groups, remain at a constant concentration. Meanwhile, the defects increase and the crystalline graphene domains reduce on GO with the increasing oxygen-containing groups. From a practical point of view, the preparation of GO is favorable at room temperature. Higher temperature brings safety problems, whereas lower temperature requires longer reaction time. Therefore, tuning the surface chemistry by adjusting the dosing of oxidation is facile and preferable. Our results provide the basis for manipulating the oxygen-containing groups on GO for its target applications.

■ ASSOCIATED CONTENT

Supporting Information

Table of XPS data which lists chemical states of C and O atoms on GO-1, GO-2, GO-3, and GO-4 with their binding energies and fwhm's. This material is available free of charge via the Internet at http://pubs.acs.org.

■ AUTHOR INFORMATION

Corresponding Author

*Fax: +86-021-64253528. Tel.: +86-021-64252169. E-mail: jhzhou@ecust.edu.cn.

Notes

The authors declare no competing financial interest.

■ ACKNOWLEDGMENTS

This work is financially supported by the Natural Science Foundation of China (21106047 and 21306046), the Fundamental Research Funds for the Central Universities (WA1214020), the Major State Basic Research Development Program of China (2014CB239702), and the China Postdoctoral Science Foundation (2012M520041 and 2013T60428).

■ REFERENCES

(1) Compton, O. C.; Nguyen, S. T. Graphene Oxide, Highly Reduced Graphene Oxide, and Graphene: Versatile Building Blocks for Carbon-Based Materials. *Small* **2010**, *6*, 711−723.

(2) Loh, K. P.; Bao, Q. L.; Eda, G.; Chhowalla, M. Graphene oxide as a chemically tunable platform for optical applications. *Nat. Chem.* **2010**, *2*, 1015−1024.

(3) Paredes, J. I.; Villar-Rodil, S.; Fernandez-Merino, M. J.; Guardia, L.; Martinez-Alonso, A.; Tascon, J. M. D. Environmentally friendly approaches toward the mass production of processable graphene from graphite oxide. *J. Mater. Chem.* **2011**, *21*, 298−306.

(4) Zhou, Y.; Bao, Q. L.; Tang, L. A. L.; Zhong, Y. L.; Loh, K. P. Hydrothermal Dehydration for the "Green" Reduction of Exfoliated Graphene Oxide to Graphene and Demonstration of Tunable Optical Limiting Properties. *Chem. Mater.* **2009**, *21*, 2950−2956.

(5) Park, S.; Ruoff, R. S. Chemical methods for the production of graphenes. *Nat. Nanotechnol.* **2009**, *4*, 217−224.

(6) Tung, V. C.; Allen, M. J.; Yang, Y.; Kaner, R. B. High-throughput solution processing of large-scale graphene. *Nat. Nanotechnol.* **2009**, *4*, 25−29.

(7) Hartono, T.; Wang, S. B.; Ma, Q.; Zhu, Z. H. Layer structured graphite oxide as a novel adsorbent for humic acid removal from aqueous solution. *J. Colloid Interface Sci.* **2009**, *333*, 114−119.

(8) Ramesha, G. K.; Kumara, A. V.; Muralidhara, H. B.; Sampath, S. Graphene and graphene oxide as effective adsorbents toward anionic and cationic dyes. *J. Colloid Interface Sci.* **2011**, *361*, 270−277.

(9) Wang, L.; Lee, K.; Sun, Y. Y.; Lucking, M.; Chen, Z. F.; Zhao, J. J.; Zhang, S. B. B. Graphene Oxide as an Ideal Substrate for Hydrogen Storage. *ACS Nano* **2009**, *3*, 2995−3000.

(10) Seredych, M.; Bandosz, T. J. Removal of ammonia by graphite oxide via its intercalation and reactive adsorption. *Carbon* **2007**, *45*, 2130−2132.

(11) Pyun, J. Graphene Oxide as Catalyst: Application of Carbon Materials beyond Nanotechnology. *Angew. Chem., Int. Ed.* **2011**, *50*, 46−48.

(12) Su, D. S.; Zhang, J.; Frank, B.; Thomas, A.; Wang, X. C.; Paraknowitsch, J.; Schlogl, R. Metal-Free Heterogeneous Catalysis for Sustainable Chemistry. *ChemSusChem* **2010**, *3*, 169−180.

(13) Machado, B. F.; Serp, P. Graphene-based materials for catalysis. *Catal. Sci. Technol.* **2012**, *2*, 54−75.

(14) (a) Petit, C.; Seredych, M.; Bandosz, T. J. Revisiting the chemistry of graphite oxides and its effect on ammonia adsorption. *J. Mater. Chem.* **2009**, *19*, 9176−9185. (b) Seredych, M.; Rossin, J. A.;

Bandosz, T. J. Changes in graphite oxide texture and chemistry upon oxidation and reduction and their effect on adsorption of ammonia. *Carbon* **2011**, *49*, 4392−4402. (c) Seredych, M.; Bandosz, T. J. Mechanism of ammonia retention on graphite oxides: Role of surface chemistry and structure. *J. Phys. Chem. C* **2007**, *111*, 15596−15604.
(15) Tang, S. B.; Cao, Z. X. Site-dependent catalytic activity of graphene oxides towards oxidative dehydrogenation of propane. *Phys. Chem. Chem. Phys.* **2012**, *14*, 16558−16565.
(16) (a) Dreyer, D. R.; Bielawski, C. W. Graphite Oxide as an Olefin Polymerization Carbocatalyst: Applications in Electrochemical Double Layer Capacitors. *Adv. Funct. Mater.* **2012**, *22*, 3247−3253. (b) Dreyer, D. R.; Jia, H. P.; Todd, A. D.; Geng, J. X.; Bielawski, C. W. Graphite oxide: a selective and highly efficient oxidant of thiols and sulfides. *Org. Biomol. Chem.* **2011**, *9*, 7292−7295. (c) Dreyer, D. R.; Jia, H. P.; Bielawski, C. W. Graphene Oxide: A Convenient Carbocatalyst for Facilitating Oxidation and Hydration Reactions. *Angew. Chem., Int. Ed.* **2010**, *49*, 6813−6816. (d) Boukhvalov, D. W.; Dreyer, D. R.; Bielawski, C. W.; Son, Y. W. A Computational Investigation of the Catalytic Properties of Graphene Oxide: Exploring Mechanisms by using DFT Methods. *ChemCatChem* **2012**, *4*, 1844−1849.
(17) Zhang, S. P.; Xiong, P.; Yang, X. J.; Wang, X. Novel PEG functionalized graphene nanosheets: enhancement of dispersibility and thermal stability. *Nanoscale* **2011**, *3*, 2169−2174.
(18) Yang, H. F.; Li, F. H.; Shan, C. S.; Han, D. X.; Zhang, Q. X.; Niu, L.; Ivaska, A. Covalent functionalization of chemically converted graphene sheets via silane and its reinforcement. *J. Mater. Chem.* **2009**, *19*, 4632−4638.
(19) Cao, Y. W.; Feng, J. C.; Wu, P. Y. Alkyl-functionalized graphene nanosheets with improved lipophilicity. *Carbon* **2010**, *48*, 1683−1685.
(20) Bai, H.; Li, C.; Shi, G. Q. Functional Composite Materials Based on Chemically Converted Graphene. *Adv. Mater.* **2011**, *23*, 1089−1115.
(21) Li, D.; Muller, M. B.; Gilje, S.; Kaner, R. B.; Wallace, G. G. Processable aqueous dispersions of graphene nanosheets. *Nat. Nanotechnol.* **2008**, *3*, 101−105.
(22) Pei, S. F.; Cheng, H. M. The reduction of graphene oxide. *Carbon* **2012**, *50*, 3210−3228.
(23) Dreyer, D. R.; Park, S.; Bielawski, C. W.; Ruoff, R. S. The chemistry of graphene oxide. *Chem. Soc. Rev.* **2010**, *39*, 228−240.
(24) Gao, W.; Alemany, L. B.; Ci, L. J.; Ajayan, P. M. New insights into the structure and reduction of graphite oxide. *Nat. Chem.* **2009**, *1*, 403−408.
(25) Nakajima, T.; Mabuchi, A.; Hagiwara, R. A new structure model of graphite oxide. *Carbon* **1988**, *26*, 357−361.
(26) Lee, D. W.; De Los Santos, L.; Seo, J. W.; Felix, L. L.; Bustamante, A.; Cole, J. M.; Barnes, C. H. W. The Structure of Graphite Oxide: Investigation of Its Surface Chemical Groups. *J. Phys. Chem. B* **2010**, *114*, 5723−5728.
(27) Szabo, T.; Berkesi, O.; Forgo, P.; Josepovits, K.; Sanakis, Y.; Petridis, D.; Dekany, I. Evolution of surface functional groups in a series of progressively oxidized graphite oxides. *Chem. Mater.* **2006**, *18*, 2740−2749.
(28) Shao, G. L.; Lu, Y. G.; Wu, F. F.; Yang, C. L.; Zeng, F. L.; Wu, Q. L. Graphene oxide: the mechanisms of oxidation and exfoliation. *J. Mater. Sci.* **2012**, *47*, 4400−4409.
(29) Mao, S.; Pu, H. H.; Chen, J. H. Graphene oxide and its reduction: modeling and experimental progress. *RSC Adv.* **2012**, *2*, 2643−2662.
(30) Boukhvalov, D. W.; Katsnelson, M. I. Modeling of graphite oxide. *J. Am. Chem. Soc.* **2008**, *130*, 10697−10701.
(31) (a) He, H.; Klinowski, J.; Forster, M.; Lerf, A. A new structural model for graphite oxide. *Chem. Phys. Lett.* **1998**, *287*, 53−56. (b) Lerf, A.; He, H.; Forster, M.; Klinowski, J. Structure of Graphite Oxide Revisited. *J. Phy. Chem. B* **1998**, *102*, 4477−4482.
(32) Hontoria-Lucas, C.; López-Peinado, A. J.; López-González, J. d. D.; Rojas-Cervantes, M. L.; Martín-Aranda, R. M. Study of oxygen-containing groups in a series of graphite oxides: Physical and chemical characterization. *Carbon* **1995**, *33*, 1585−1592.
(33) De La Cruz, F. A.; Cowley, J. M. Structure of Graphitic Oxide. *Nature* **1962**, *196*, 468−469.
(34) Botas, C.; Alvarez, P.; Blanco, C.; Santamaria, R.; Granda, M.; Ares, P.; Rodriguez-Reinoso, F.; Menendez, R. The effect of the parent graphite on the structure of graphene oxide. *Carbon* **2012**, *50*, 275−282.
(35) He, H.; Riedl, T.; Lerf, A.; Klinowski, J. Solid-State NMR Studies of the Structure of Graphite Oxide. *J. Phys. Chem.* **1996**, *100*, 19954−19958.
(36) Wang, H.; Hu, Y. H. Effect of Oxygen Content on Structures of Graphite Oxides. *Ind. Eng. Chem. Res.* **2011**, *50*, 6132−6137.
(37) Kovtyukhova, N. I.; Ollivier, P. J.; Martin, B. R.; Mallouk, T. E.; Chizhik, S. A.; Buzaneva, E. V.; Gorchinskiy, A. D. Layer-by-layer assembly of ultrathin composite films from micron-sized graphite oxide sheets and polycations. *Chem. Mater.* **1999**, *11*, 771−778.
(38) Stankovich, S.; Piner, R. D.; Nguyen, S. T.; Ruoff, R. S. Synthesis and exfoliation of isocyanate-treated graphene oxide nanoplatelets. *Carbon* **2006**, *44*, 3342−3347.
(39) Titelman, G. I.; Gelman, V.; Bron, S.; Khalfin, R. L.; Cohen, Y.; Bianco-Peled, H. Characteristics and microstructure of aqueous colloidal dispersions of graphite oxide. *Carbon* **2005**, *43*, 641−649.
(40) Casablanca, L. B.; Shaibat, M. A.; Cai, W. W. W.; Park, S.; Piner, R.; Ruoff, R. S.; Ishii, Y. NMR-Based Structural Modeling of Graphite Oxide Using Multidimensional C-13 Solid-State NMR and ab Initio Chemical Shift Calculations. *J. Am. Chem. Soc.* **2010**, *132*, 5672−5676.
(41) Cai, W. W.; Piner, R. D.; Stadermann, F. J.; Park, S.; Shaibat, M. A.; Ishii, Y.; Yang, D. X.; Velamakanni, A.; An, S. J.; Stoller, M.; An, J. H.; Chen, D. M.; Ruoff, R. S. Synthesis and solid-state NMR structural characterization of ^{13}C-labeled graphite oxide. *Science* **2008**, *321*, 1815−1817.
(42) Liu, Z. T.; Duan, X. Z.; Qian, G.; Zhou, X. G.; Yuan, W. K. Eco-friendly one-pot synthesis of highly dispersible functionalized graphene nanosheets with free amino groups. *Nanotechnology* **2013**, *24*, 045609.
(43) Zarrin, H.; Higgins, D.; Jun, Y.; Chen, Z. W.; Fowler, M. Functionalized Graphene Oxide Nanocomposite Membrane for Low Humidity and High Temperature Proton Exchange Membrane Fuel Cells. *J. Phys. Chem. C* **2011**, *115*, 20774−20781.
(44) Wang, H. L.; Robinson, J. T.; Li, X. L.; Dai, H. J. Solvothermal Reduction of Chemically Exfoliated Graphene Sheets. *J. Am. Chem. Soc.* **2009**, *131*, 9910−9911.
(45) Xue, T. Y.; Cui, X. Q.; Chen, J. L.; Liu, C.; Wang, Q. Y.; Wang, H. T.; Zheng, W. T. A Switch of the Oxidation State of Graphene Oxide on a Surface Plasmon Resonance Chip. *ACS Appl. Mater. Interfaces* **2013**, *5*, 2096−2103.
(46) Chen, J. L.; Zhang, X. M.; Zheng, X. L.; Liu, C.; Cui, X. Q.; Zheng, W. T. Size distribution-controlled preparation of graphene oxide nanosheets with different C/O ratios. *Mater. Chem. Phys.* **2013**, *139*, 8−11.